GJB2 as a Novel Prognostic Biomarker Associated with Immune Infiltration and Cuproptosis in Ovarian Cancer

Han Lei[1], Ke Guo[3], Guang Shu[1], Maonan Wang[1], Yu Li[4], Zhihui Tan[5*], Qiong Pan[2*], Gang Yin[1,6,7*]

[1] Department of Pathology, Xiangya Hospital, School of Basic Medical Sciences, Central South University, Changsha, China.

[2] Department of Obstetrics and Gynecology, The Third Xiangya Hospital of Central South University, Changsha, China.

[3] Department of Neurology, The Third Xiangya Hospital of Central South University, Changsha, China.

[4] Intensive Care Unit for Children, Xiangtan Central Hospital, China.

[5] Department of Gynecology, Xiangya Hospital, Central South University, Changsha, China.

[6] China-Africa Research Center of Infectious Diseases, School of Basic Medical Sciences, Central South University, Changsha, China.

[7] National Clinical Research Center for Geriatric Disorders, Xiangya Hospital, Central South University, Changsha, China.

[*] Corresponding author: Zhihui Tan, tanzhihui@csu.edu.cn; Qiong Pan, 1517682924@qq.com; Gang Yin, gangyin@csu.edu.cn.

Supplementary Materials

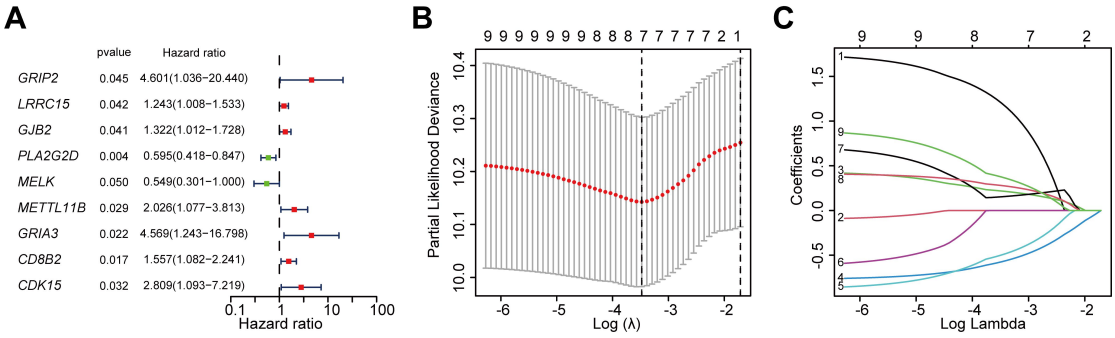

Fig. S1 Construction of the CRGs Prognostic Signature in OC

(A) The univariate Cox regression analysis between CRGs and OS of OCs is shown in the forest plots. The P-values were obtained by univariate Cox regression. **(B)** LASSO regression with 10-fold cross-validation obtained 7 prognostic genes using the minimum Lambda. **(C)** LASSO coefficient profile of candidate genes.

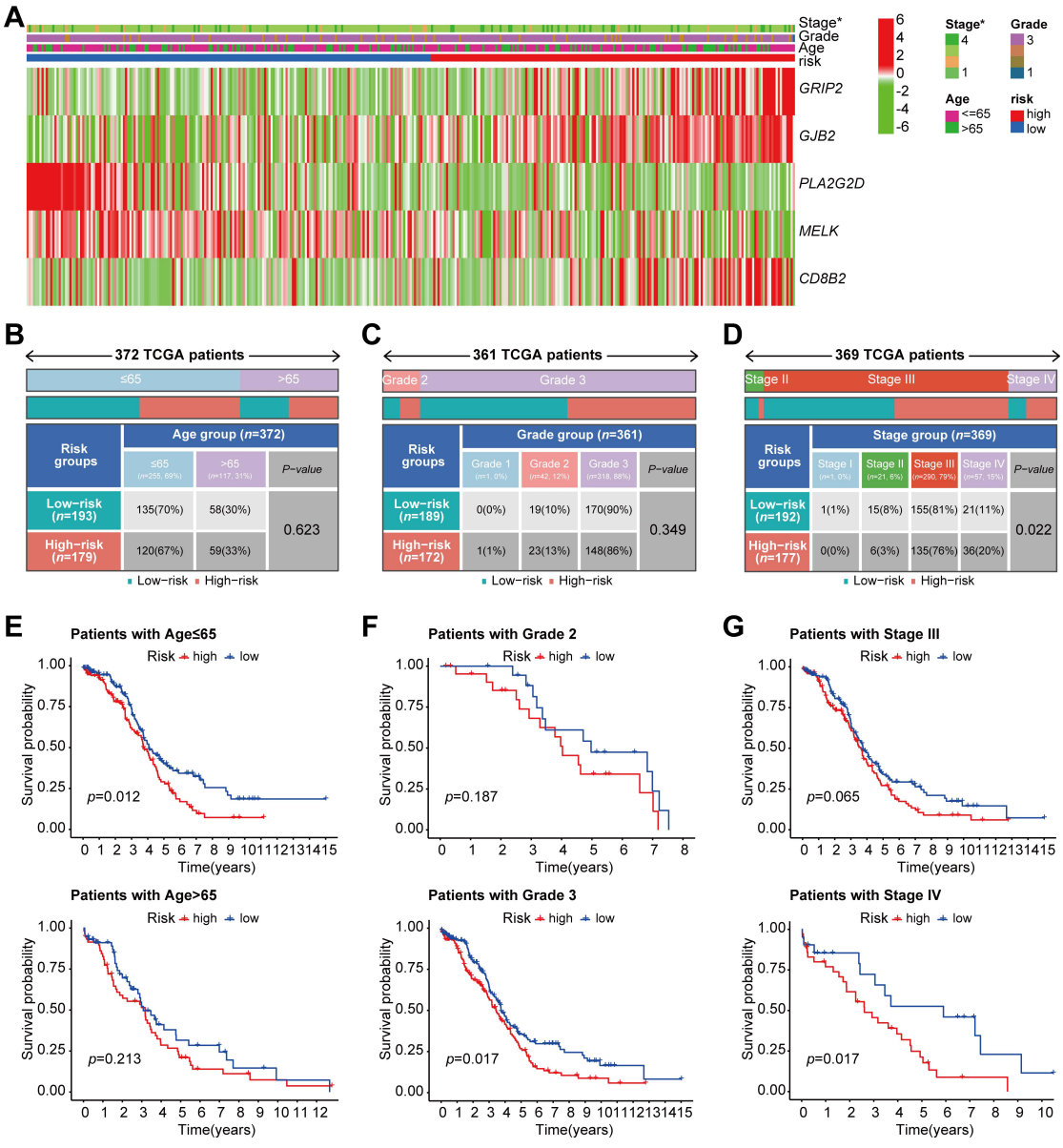

Fig. S2 Heatmap and KM Curves of Clinicopathological Variables in the High-risk and Low-risk Groups

(A) Heatmap for CRGs prognostic signature and clinicopathological manifestations. **(B-D)** Distribution of Age **(B)**, Grade **(C)**, and Stage **(D)** clinicopathological variables in high-risk and low-risk groups. **(E-G)** KM survival curves of Age **(E)**, Grade **(F)**, and Stage **(G)** clinicopathological variables in the high-risk and low-risk groups.

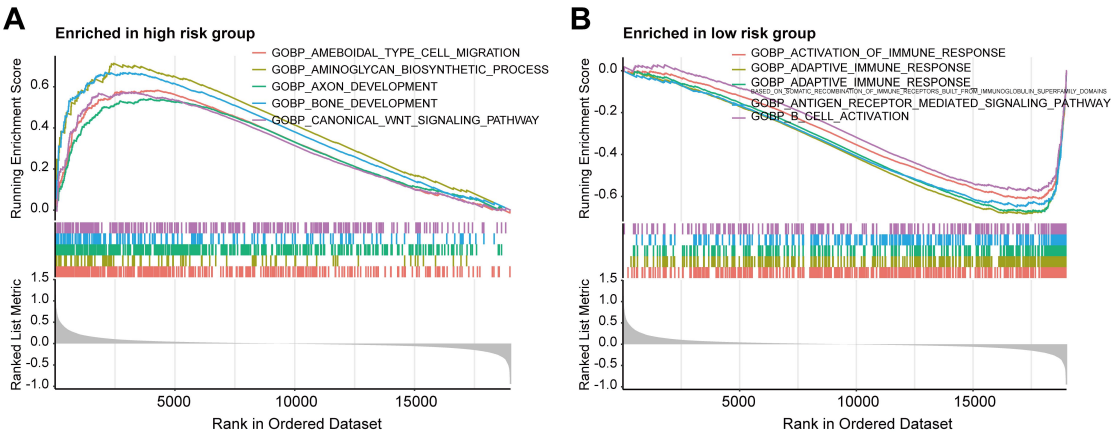

Fig. S3 GSEA Enrichment Analysis (GO) between the High-risk and Low-risk Groups

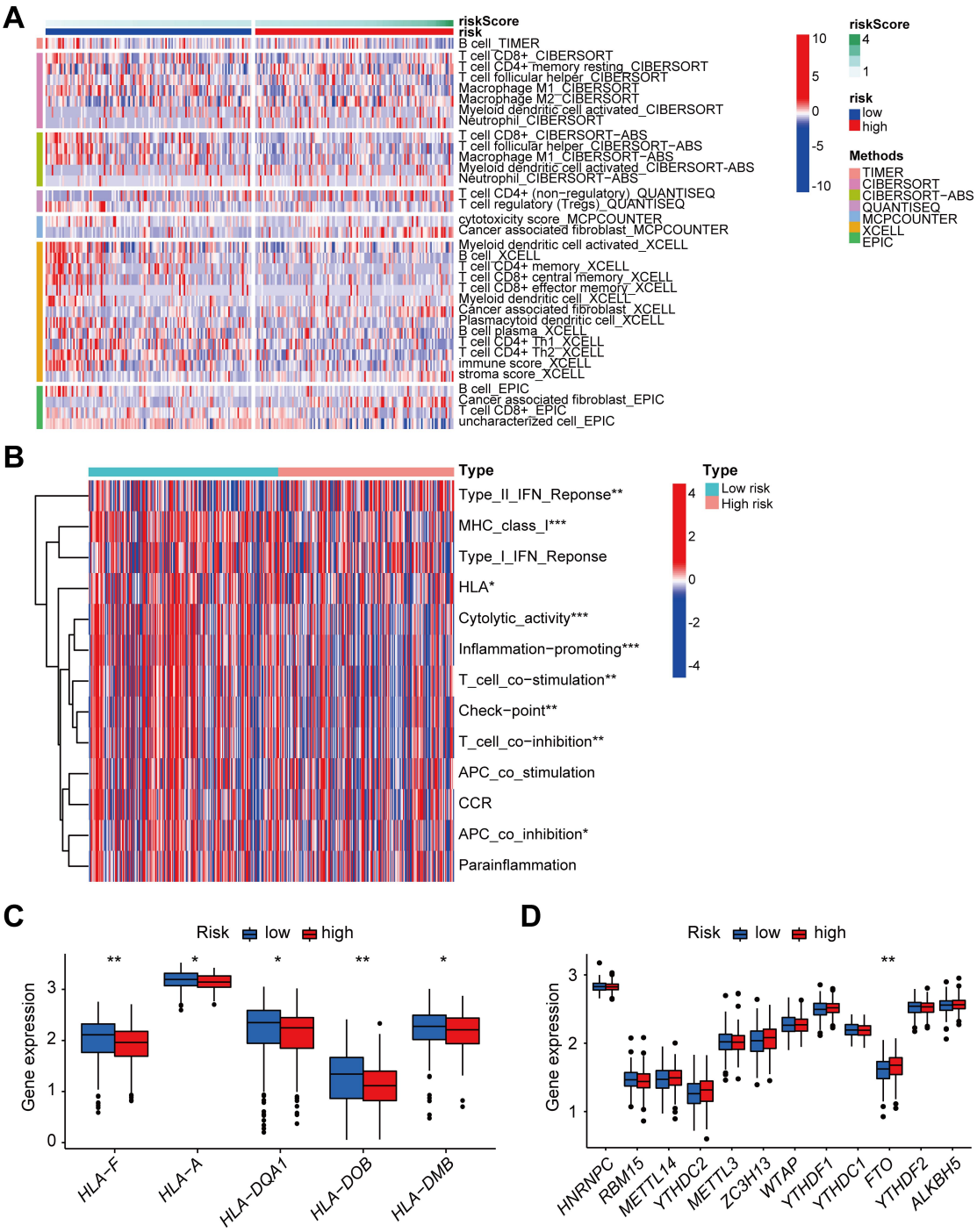

Fig. S4 Correlation Analysis between High/Low-risk Groups and Immunity

(A) A heatmap of all substantially distinct immune cells between the high-risk and low-risk score subgroups. **(B)** The correlation between the predictive signature and 13 immune-related functions. **(C)** Differential expression of HLA-related indicators. **(D)** Differential expression of m6A-related genes.

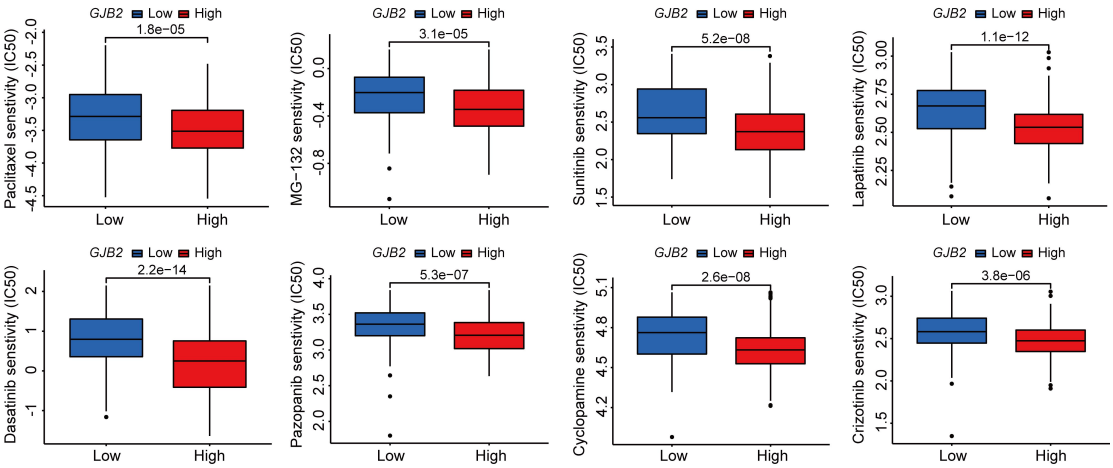

Fig. S5 Drug Sensitivity (IC50) Correlated with the High-expression and Low-expression Groups of *GJB2* in OC Patients

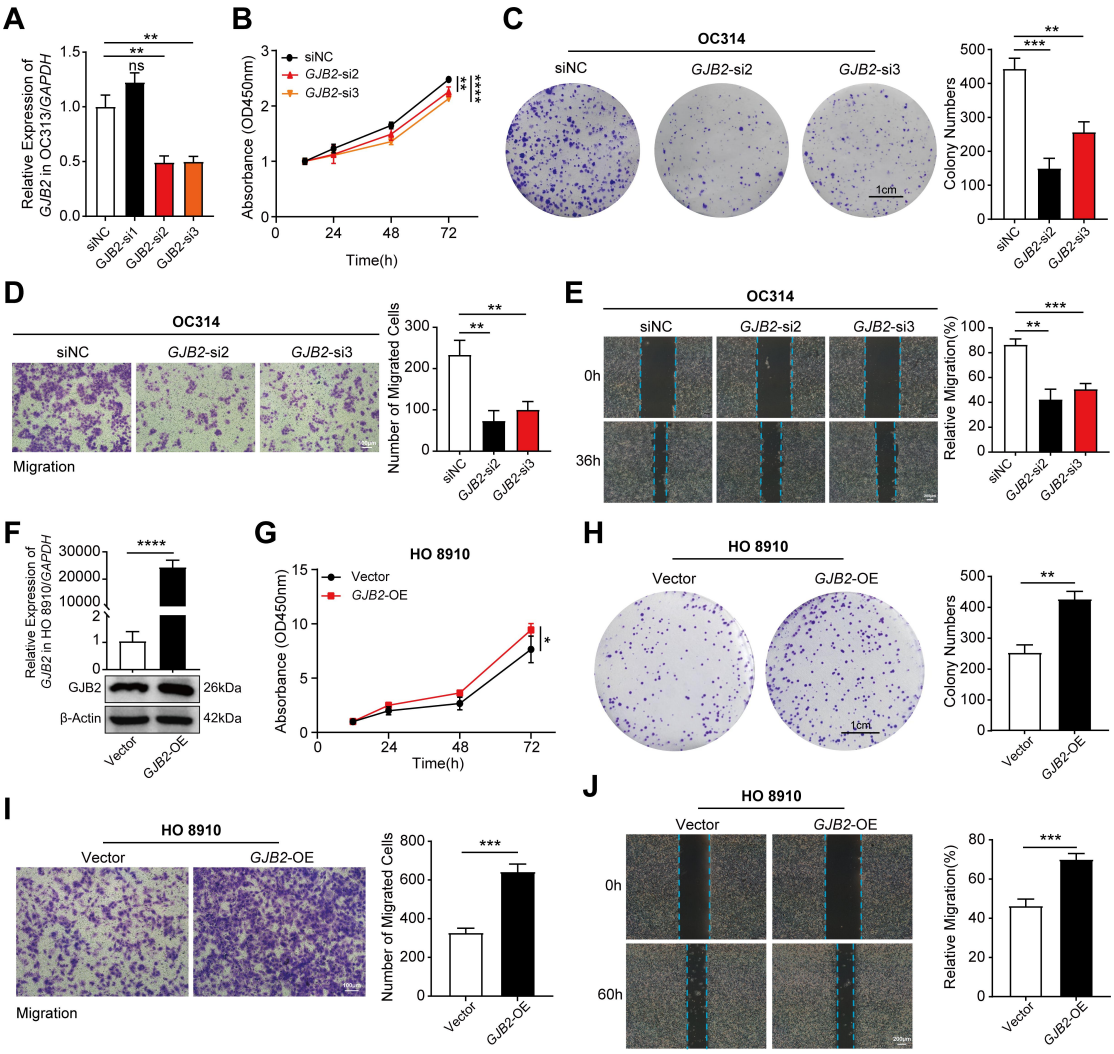

Fig. S6 Influence of Abnormal Expression of *GJB2* on Cell Proliferation and Migration in OC

(A) The transfection efficiency of *GJB2* siRNA in OC314 was detected by qPCR. **(B)** The CCK-8 assay showed that *GJB2* interference significantly inhibited OC314 cell proliferation at 12, 24, 48, and

72 h. **(C)** Knockdown of *GJB2* inhibited the proliferation ability of OC314 cells and was evaluated by a colony formation assay. **(D-E)** Transwell **(D)** and wound healing **(E)** assays were performed to determine the effect of *GJB2* knockdown on the migration ability of OC314 cells. **(F)** Validation of *GJB2* expression after transfection of *GJB2*-OE and negative control (NC) plasmids in HO 8910 cells using qPCR and Western blotting assays. **(G-H)** The CCK-8 **(G)** and colony formation **(H)** assay display the effect of *GJB2* upregulation on HO 8910 cell proliferation ability. **(I-J)** The effects of *GJB2*-OE on HO 8910 cell migration were evaluated through Transwell **(I)** and wound healing **(J)** assays. In all statistical plots, data are expressed as the mean ± SD. *$p<0.05$, **$p<0.01$, ***$p<0.001$, ****$p<0.0001$.